Bath-Induced Zeno Localization in Driven Many-Body Quantum Systems

Thibaud Maimbourg,[1,*] Denis M. Basko,[2] Markus Holzmann,[2] and Alberto Rosso[1]
[1]LPTMS, CNRS, Université Paris-Saclay, 91405 Orsay, France
[2]Université Grenoble Alpes and LPMMC, CNRS, 25 rue des Martyrs, 38042 Grenoble, France

(Received 2 October 2020; accepted 22 February 2021; published 23 March 2021)

We study a quantum interacting spin system subject to an external drive and coupled to a thermal bath of vibrational modes, uncorrelated for different spins, serving as a model for dynamic nuclear polarization protocols. We show that even when the many-body eigenstates of the system are ergodic, a sufficiently strong coupling to the bath may effectively localize the spins due to many-body quantum Zeno effect. Our results provide an explanation of the breakdown of the thermal mixing regime experimentally observed above 4–5 K in these protocols.

DOI: 10.1103/PhysRevLett.126.120603

The thermalization of an isolated many-body quantum system stems from two mechanisms. The first is dephasing, i.e., the projection by the unitary dynamics of the initial state onto the Hamiltonian eigenstates. The second is the matching between the expectation value of physical observables in these eigenstates and those of the microcanonical ensemble. This second property, called the eigenstate thermalization hypothesis (ETH) [1–4], implies that if the quantum state is a mixture of Hamiltonian eigenstates, the system appears thermal. Consequently, one expects that even in the presence of a drive and dissipation, a unique effective temperature characterizes the stationary state [5–9].

A celebrated confirmation of this scenario is the *thermal mixing* reached in dynamic nuclear polarization (DNP) [5,10], a protocol used for NMR applications. A sample, doped with molecules possessing unpaired electron spins, is exposed to a strong magnetic field, frozen at temperature $\beta^{-1} \sim 1$ K and driven out of equilibrium by microwave irradiation at frequency ω_{MW}. After one hour all nuclear species in the sample (^{1}H, ^{13}C, ^{15}N…) thermalize to a single temperature β_s^{-1}, called spin temperature [10,11]. By tuning ω_{MW}, one can reach $\beta_s \gg \beta$, which strongly hyperpolarizes the nuclear spins, an essential aim in NMR spectrometry and imaging. Inconveniently, this regime disappears above 4–5 K and nuclear polarization becomes weak [12–14].

In this Letter, we show how a coupling to a local bath can explain the thermal mixing breakdown and reveal fingerprints of localization in this nonequilibrium steady state. Such ergodicity breaking is not caused by a violation of ETH, as in strongly disordered systems—a phenomenon called many-body localization (MBL) [15–19]—but by a competition between dephasing and system-bath interaction that prevents the stationary state from being an eigenstate mixture. This phenomenon is a many-body analog of the quantum Zeno effect [20–26], where infinitely frequent measurements impede the unitary evolution of a single degree of freedom. Here the interaction with bath modes, uncorrelated for different spins, plays the role of the measurements. We show that going beyond the traditional scheme of weak coupling to the bath [5–9,27], through a recently proposed approach not relying on the secular approximation [28–30], is necessary to account for this type of localization.

The DNP arises from the steady state of N unpaired electron spins. Their Hamiltonian reads [Fig. 1(a)]

$$\hat{H}_S = \sum_{i=1}^{N} (\omega_e + \Delta_i)\hat{S}_i^z + \hat{H}_{\mathrm{dip}}. \tag{1}$$

ω_e is the strong magnetic field along the z axis (Zeeman gap). Δ_i is a small disorder from the random orientation of the molecule where the spin lies and $\hat{H}_{\mathrm{dip}}$ stands for the dipolar interaction. The large magnetic field implies $\hat{S}^z = \sum_i \hat{S}_i^z$ is conserved; hence the dipolar Hamiltonian gets truncated as [6,10,31,32]

$$\hat{H}_{\mathrm{dip}} = \sum_{i<j} U_{ij}(\hat{S}_i^+\hat{S}_j^- + \hat{S}_i^-\hat{S}_j^+ - 4\hat{S}_i^z\hat{S}_j^z), \tag{2}$$

where U_{ij} depends on the distance between the spins and their orientation with respect to the magnetic field. The spins are in contact with a thermal bath and driven by microwaves through $\hat{H}_{\mathrm{MW}}(t) = \omega_1[\hat{S}^x\cos(\omega_{\mathrm{MW}}t) + \hat{S}^y\sin(\omega_{\mathrm{MW}}t)]$. When $\omega_{\mathrm{MW}} \approx \omega_e$, the electron spins reach a stationary state probed experimentally by measuring the electron paramagnetic resonance (EPR) spectrum. Two typical shapes can occur: (i) A linear curve close to irradiation frequency [Fig. 1(b)]. Electrons are in thermal mixing, i.e., equilibrated at the spin temperature β_s^{-1} and interacting via $\hat{H}_S$ with a shifted magnetic field $\omega_e \to \omega_e - h$, where $h \simeq \omega_{\mathrm{MW}}$. Through hyperfine interaction with the electron spins, the nuclear spins thermalize with polarization $P_n = \tanh(\beta_s\omega_n/2)$ (ω_n is

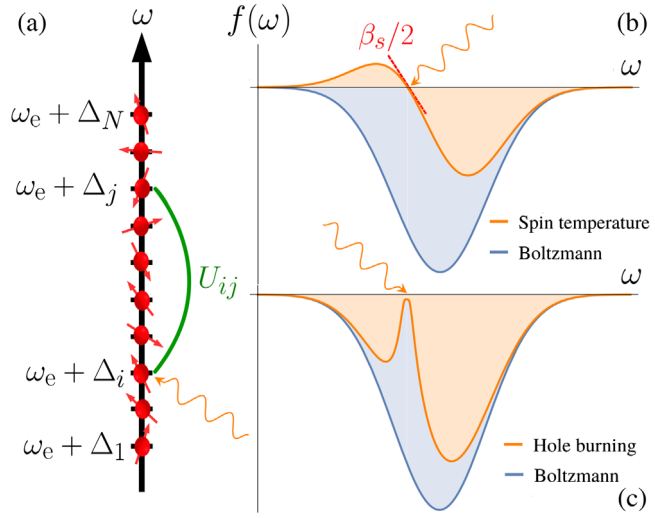

FIG. 1. (a) Sketch of the system: N electron spins with dipolar interactions of strength U_{ij} in a strong inhomogeneous magnetic field $\omega_e + \Delta_i$ in contact with a thermostat are irradiated by microwaves at frequency $\omega_{\rm MW}$ (wavy arrow). (b),(c) EPR spectrum $f(\omega)$ [defined via Eq. (11)] at Boltzmann equilibrium (blue curve) and under microwave driving displaying two shapes (orange curves). (b) The spin-temperature profile [10,34] with linear behavior (dashed red line) of slope $\beta_s/2$ close to resonance $\omega = \omega_{\rm MW}$. (c) The hole burning at resonance.

the nuclear Zeeman gap) [5,6,10]. (ii) A "hole burning" close to irradiation [Fig. 1(c)] found by Bloch [33] for non-interacting spins: the resonant spins ($\omega_e + \Delta_i \simeq \omega_{\rm MW}$) are brought to a high temperature while off-resonant ones remain at β^{-1}. The hole-burning shape is recovered in the MBL regime [5–8,27], revealing different local temperatures: the nuclear species exhibit weak polarization not accounted for by a single temperature.

The spin-temperature shape was observed long ago in the EPR spectrum of Ce^{3+} in $CaWO_4$ crystals [34]. More recently, experiments on irradiated EPR spectrum retrieved instead a hole-burning shape [12–14] above 4–5 K. In the following, we argue that even in ETH systems, a bath of uncorrelated modes triggers quantum jumps that can induce localization if bath transitions prevail over dephasing. In particular, we compute the EPR spectrum and show a crossover from a spin-temperature to a hole-burning shape. We interpret this crossover as a manifestation of a bath-induced Zeno localization in the many-body eigenbasis of $\{\hat{S}_i^z\}$. As bath transitions become more effective when raising temperature, curiously, this ergodicity breaking happens in the high-temperature phase.

Effective dynamics due to the bath.—The electron spins are dilute, so we assume they are in contact with vibration modes $\hat{B}_i^\mu$ [35], Sec. V, that are uncorrelated (thus they cannot induce effective interactions between spins):

$$\hat{H}_{\rm int} = \sum_{\substack{i=1,\ldots,N \\ \mu=x,y,z}} \hat{S}_i^\mu \otimes \hat{B}_i^\mu. \tag{3}$$

Assuming the bath is equilibrated at temperature β^{-1}, we trace out the $\hat{B}_i^\mu$ variables in the full density matrix $\rho_{S\otimes B}$ and write an effective evolution for the spin system density matrix $\rho = {\rm Tr}_B(\rho_{S\otimes B})$. The ensuing evolution is no longer unitary but must still preserve the trace and semipositivity of ρ. The most general Markovian dynamics must then be of the Gorini-Kossakowski-Sudarshan-Lindblad (GKSL) form [25]:

$$\dot{\rho} = -i[\hat{H}, \rho] + \sum_\alpha \hat{A}_\alpha \rho \hat{A}_\alpha^\dagger - \frac{1}{2}\{\hat{A}_\alpha^\dagger \hat{A}_\alpha, \rho\}, \tag{4}$$

where $\hat{H}$ is Hermitian and $\{\hat{A}_\alpha\}$ is a set of jump operators. To integrate the bath degrees of freedom [35], Sec. I, we consider weak spin-bath coupling and perform a perturbative expansion of the full unitary dynamics of $\rho_{S\otimes B}$ at second order in $\hat{H}_{\rm int}$. The Born-Markov approximation [25,48,49] yields an effective Markovian evolution for ρ. The uncorrelated bath degrees of freedom are described by a single equilibrium correlation function

$$\gamma(\omega) = \int_{-\infty}^{\infty} d\tau e^{i\omega\tau} \langle \hat{B}_i^\mu(\tau) \hat{B}_i^\mu(0) \rangle_B = \frac{h(\omega)}{T(|\omega|)}, \tag{5}$$

where $h(\omega) = (1 + e^{-\beta\omega})^{-1}$ enforces detailed balance, while $T(|\omega|)$ is the timescale of energy exchange ω with the spins.

The Markovian approximation is not unique and in general not in GKSL form (4). We implement the Markovian prescription of [28–30], which leads to a GKSL form setting $\hat{H} = \hat{H}_S$ and

$$\hat{A}_\alpha = \sum_{n,m} \sqrt{\gamma(\omega_{nm})} \langle m|\hat{S}_i^\mu|n\rangle |m\rangle\langle n|, \tag{6}$$

with $\alpha = (i, \mu)$ and $\omega_{nm} = \varepsilon_n - \varepsilon_m$ are $\hat{H}_S$ energy gaps. We have three typical timescales $T(|\omega|)$: (i) T_1 for transitions of energy gap $\pm\omega_e$, giving the jump operators

$$\hat{A}_i^x = \sqrt{\frac{h(\omega_e)}{2T_1}}(\hat{S}_i^- + e^{-\beta\omega_e/2}\hat{S}_i^+),$$
$$\hat{A}_i^y = i\sqrt{\frac{h(\omega_e)}{2T_1}}(\hat{S}_i^- - e^{-\beta\omega_e/2}\hat{S}_i^+) \tag{7}$$

(ii) T^* for transitions of finite energy $|\omega| \ll \omega_e$, and (iii) $T(0)$ for zero-energy transitions within the same eigenstate, giving

$$\hat{A}_i^z = \frac{\hat{S}_i^z}{\sqrt{2T^*}} + \left(\frac{1}{\sqrt{2T(0)}} - \frac{1}{\sqrt{2T^*}}\right) \sum_n \langle n|\hat{S}_i^z|n\rangle |n\rangle\langle n|. \tag{8}$$

The nonsecular jump operators (7), (8) [when $T(0) \approx T^*$] are well localized in space. The quantum trajectories result

from a competition between the unitary dynamics projecting on thermal eigenstates and repeated measurements performed by the nonsecular jump operators. If jump rates dominate, thermalization is hampered in a way reminiscent of the quantum Zeno effect.

This choice of jump operators contrasts with the usual weak-coupling prescription [25,48,49], where a GKSL [Eq. (4)] is recovered through an additional secular approximation. The jump operators select only a given transition energy ω_{nm} between eigenstates $|m\rangle$ and $|n\rangle$:

$$\hat{A}^{\mathrm{sec}}_{\alpha}(\omega_{nm}) = \sqrt{\gamma(\omega_{nm})}\langle m|\hat{S}^{\mu}_{i}|n\rangle|m\rangle\langle n|. \tag{9}$$

The secular jump operators (9) are directly projected on the eigenstates of $\hat{H}_S$, unlike jumps (7), (8), for which the secular approximation is released. With these nonsecular jumps, the system's state gets projected on the Hamiltonian eigenstates only if bath timescales T_1, T^* are long with respect to dephasing. To emphasize the effect of the secular approximation, we insert Eq. (9) into Eq. (4), yielding an exponential decay of the off-diagonal elements (coherences) in the eigenbasis:

$$\dot{\rho}_{nm} = -\left(i\omega_{nm} + \frac{1}{T_{nm}}\right)\rho_{nm}, \tag{10}$$

where $i\omega_{nm}$ is the dephasing due to the unitary evolution and $T_{nm} > 0$ is the decoherence [35], Sec. I B originating from the bath timescales. Therefore one can work in the Hilbert approximation where the dynamics is projected on the diagonal elements: it amounts to transit from one eigenstate to the other with rates given in [35], Sec. I E. The nonsecular dynamics (6) adds to the right-hand side of Eq. (10) entries other than ρ_{nm}, with associated bath rates [35], Sec. I F, allowing the existence of steady-state coherences.

Microwave drive.—In equilibrium, the steady state is in practice accurately described by the Boltzmann distribution with either choice of jump operators [28,50,51]. The nonsecular evolution brings drastic changes out of equilibrium: the drive creates an imbalance that probes localization. In a DNP protocol the system is irradiated by microwaves described by $\hat{H}_{\mathrm{MW}}(t)$. They induce local temperature inhomogeneities as resonant spins get hotter while others are frozen by the low-temperature bath. The dynamics of the rotating-frame density matrix $e^{i\omega_{\mathrm{MW}}t\hat{S}^z}\rho(t)e^{-i\omega_{\mathrm{MW}}t\hat{S}^z} \to \rho(t)$ remains given by Eq. (4) with the shift $\hat{H} = \hat{H}_S - \omega_{\mathrm{MW}}\hat{S}^z + \omega_1\hat{S}^x$ [35], Sec. I D.

Numerical computation of the EPR spectrum.—We compare the stationary states predicted by the Hilbert dynamics with the ones obtained by the nonsecular evolution Eq. (4) with jumps (7), (8) for uniform disorder $\Delta_i \in [-(\Delta\omega_e/2), (\Delta\omega_e/2)]$ and U_{ij} mimicked by independent Gaussian distributions with zero mean and variance U^2/N. We fix $\Delta\omega_e = 5 \times 2\pi$ MHz, $U = 0.75 \times 2\pi$ MHz (note that $\omega_e = 93.9 \times 2\pi$ GHz), where $\hat{H}_S$ has ETH statistics. We consider two temperatures; at high temperature the bath timescales are short (Table I).

TABLE I. Control parameters chosen for the system at two temperatures, close to experimental values [5,14,52].

β^{-1} (K)	$T(0)$ (μs)	T^* (μs)	T_1 (μs)	ω_1 (2π MHz)	ω_{MW} (2π GHz)
1.2	1.6	80	160	0.628	93.8988
12	0.16	0.16	1.6	0.628	93.8988

We compute numerically the steady-state density matrix ρ_{stat} [53]. The Hilbert case amounts to a $2^N \times 2^N$ linear system, which for $N = 10$ spins is treated by exact diagonalization. The nonsecular dynamics Eq. (4) is instead a $4^N \times 4^N$ linear system requiring Krylov subspace methods (biconjugate gradient-stabilized algorithm) [54]. To probe the stationary state we focus on the EPR spectrum: starting at time $\tau = 0$, a $\pi/2$ microwave pulse projects the steady-state polarization of a given spin i on the y axis,respect to both dephasing time $\rho_{\pi/2} = e^{i(\pi/2)\hat{S}^x_i}\rho_{\mathrm{stat}}e^{-i(\pi/2)\hat{S}^x_i}$. For short times

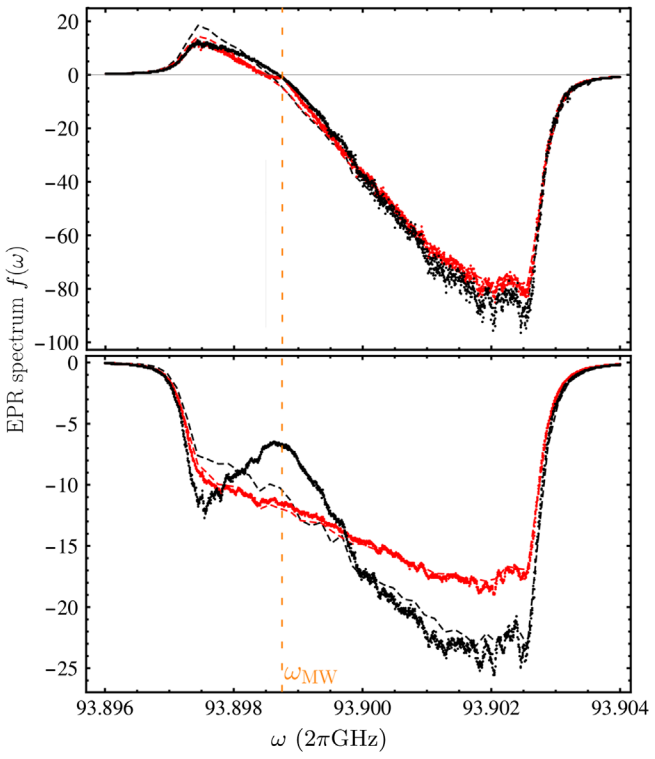

FIG. 2. EPR spectra: dots represent numerical profiles for Hilbert (red) and nonsecular (black) evolutions. Dashed lines are calculated through a spin-temperature ansatz. Top: $\beta^{-1} = 1.2$ K. The bath is slow, nonsecular and Hilbert dynamics provide analogous spin-temperature curves. Bottom: $\beta^{-1} = 12$ K. Bath timescales are short, the nonsecular dynamics gets localized and displays a hole burning. Here the Hilbert approximation fails, predicting a spin-temperature behavior. Averages are done over 1000 realizations.

after the pulse, the evolution is unitary and the polarization in the (x, y) plane is encoded in

$$g_i(\tau) = -2i\mathrm{Tr}[\hat{S}_i^+(\tau)\rho_{\pi/2}], \tag{11}$$

where $\hat{S}_i^+(\tau) = e^{i\hat{H}_S\tau}\hat{S}_i^+e^{-i\hat{H}_S\tau}$. The EPR spectrum is defined by Fourier transform: $f(\omega)=1/N\sum_i \mathrm{Re}[\int_0^\infty d\tau/\pi g_i(\tau)e^{-i\omega\tau}]$ [35], Sec. II.

At low temperature, we observe a spin-temperature curve for both dynamics in the EPR spectra (Fig. 2). Here the bath timescales T^*, T_1 are long with respect to both dephasing time $\omega_{nm}^{-1} \approx \min(1/U, 1/\Delta\omega_e)$ and decoherence time $T_{nm} \approx T(0)$. Consequently, the density matrix gets projected in the eigenstate basis, as in the Hilbert approximation. At higher temperature, the EPR spectrum is spin-temperature-like for Hilbert dynamics, whereas it has a hole-burning shape in the nonsecular evolution. The spin-temperature behavior observed in the Hilbert approximation is expected [5,6,27]: due to ETH, the jump operators projected on eigenstates generate energy and polarization changes without any other information such as the spatial location of the spins. Conversely, in the nonsecular equation the jump operators are well localized in space and compete with dephasing, which is unable to project the system on the eigenstates (as T^* becomes comparable to dephasing and decoherence times). The EPR spectrum develops a hole burning similar to the one already observed when $\hat{H}_S$ has MBL eigenstates [5,6] and [35], Fig. S3, although $\hat{H}_S$ eigenstates are ergodic for our parameters. This breakdown is confirmed by comparing the EPR profiles with the ones (dashed lines in Fig. 2) obtained through a spin-temperature ansatz for the steady-state density

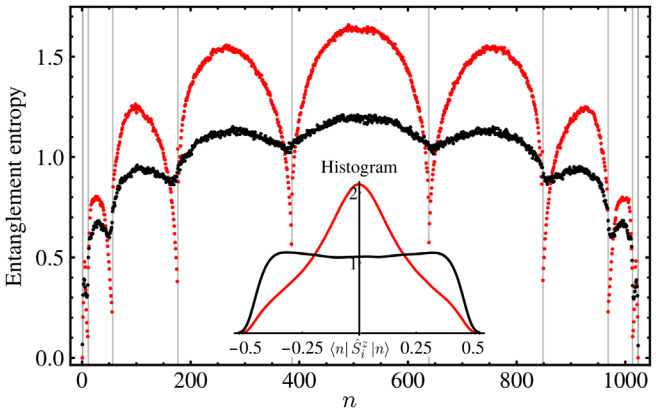

FIG. 3. Entanglement entropy of ρ_{stat}'s eigenstates (Hilbert, red; nonsecular, black) classified by increasing energy, computed through partial trace of each eigenstate $|n\rangle\langle n|$ over spins 5 to 10. Vertical lines delimit polarization sectors. Inset: Smoothed histogram of S_i^z expectation values ($i = 1, \ldots, N$) for 100 eigenstates in the middle of the $s_n^z = 0$ sector. For the Hamiltonian eigenstates, the observable is peaked around $S_i^z \simeq 0$, as required by ETH. The nonsecular eigenstates present instead strong fluctuations, as for MBL states. Parameters are those of Fig. 2 (bottom).

matrix $\rho_{nn}^{\mathrm{ans}}(\beta_s, h) \propto e^{-\beta_s(\epsilon_n - hs_n^z)}$. s_n^z are eigenvalues of the conserved $\hat{S}^z$. The spin temperature β_s^{-1} (respectively magnetic field h) is conjugated to the energy (respectively polarization) and determined by a fit [6] and [35], Sec. III B

Spectral properties.—The localization phenomenon exhibited by the experimentally relevant EPR spectra is revealed through other observables, e.g., polarization profiles [35], Sec. III. In Fig. 3, we compare the entanglement entropy of the ρ_{stat} eigenstates in the Hilbert and nonsecular cases. The latter case is much less entangled and similar to MBL eigenstates [35], Sec. III D, where Fig. S7 shows a fully localized case. The present scenario is akin to the measurement-induced entanglement transition in schematic models such as quantum circuits [55–63], free fermionic chains [64] and interacting bosonic chains [65–67].

Discussion and conclusion.—In open systems the external bath permits thermalization even for strong disorder, when eigenstates are localized. This is manifested by phonon-induced hopping transport [68]: the bath supplies or absorbs the energy needed to hop between localized states. Here, we have shown how coupling to uncorrelated thermal vibrations can instead induce localization in quantum many-body systems with ergodic eigenstates, revealed in presence of a drive. Whether this is a sharp transition or a smooth crossover in the thermodynamic limit remains an intriguing open question. Going beyond the conventional secular approximation [25] is required to capture this phenomenon. The mechanism underlying this many-body Zeno effect is distinct from the Zeno effect in quantum gases with localized particle losses [69–72] or dephasing [73], where the combined impact of local single-particle losses and interactions renormalizes single-particle quantities. It also differs from localization by subohmic baths at zero temperature [74–77], a polaronic effect wiped out by interactions or temperature [78]. In the DNP context, our work, based on heuristic values of the microscopic timescales, provides an explanation for the thermal-mixing breakdown upon increasing temperature, arising from enhanced dynamics of the vibrational modes. The present analysis calls for a thorough experimental test of temperature influence on the different hyperpolarization regimes.

We thank Fabien Alet, Leticia Cugliandolo, Andrea De Luca, Laura Foini, Nicolas Laflorencie, Leonardo Mazza, and Marco Schiró for valuable discussions around different facets of this work. We also are grateful to Filippo Vicentini for advices on the numerical methods. We acknowledge funding from the grant THERMOLOC ANR-16-CE30-0023-01 and the Galileo Galilei Institute for hospitality during part of this project.

*thibaud.maimbourg@lptms.u-psud.fr

[1] E. M. Lifshitz and L. P. Pitaevskii, *Statistical Physics, Part 2*, edited by L. D. Landau and E. M. Lifshitz, Course of

Theoretical Physics Vol. 9 (Pergamon Press, New York, 1980), Sec. 41.
[2] J. M. Deutsch, Phys. Rev. A **43**, 2046 (1991).
[3] M. Srednicki, Phys. Rev. E **50**, 888 (1994).
[4] L. D'Alessio, Y. Kafri, A. Polkovnikov, and M. Rigol, Adv. Phys. **65**, 239 (2016).
[5] A. De Luca and A. Rosso, Phys. Rev. Lett. **115**, 080401 (2015).
[6] A. De Luca, I. R. Arias, M. Müller, and A. Rosso, Phys. Rev. B **94**, 014203 (2016).
[7] Z. Lenarčič, E. Altman, and A. Rosch, Phys. Rev. Lett. **121**, 267603 (2018).
[8] Z. Lenarčič, O. Alberton, A. Rosch, and E. Altman, Phys. Rev. Lett. **125**, 116601 (2020).
[9] F. Lange, Z. Lenarčič, and A. Rosch, Nat. Commun. **8**, 15767 (2017).
[10] A. Abragam, *The Principles of Nuclear Magnetism*, Vol. 32 (Oxford University Press, New York, 1961).
[11] D. Guarin, S. Marhabaie, A. Rosso, D. Abergel, G. Bodenhausen, K. L. Ivanov, and D. Kurzbach, J. Phys. Chem. Lett. **8**, 5531 (2017).
[12] P. Schosseler, T. Wacker, and A. Schweiger, Chem. Phys. Lett. **224**, 319 (1994).
[13] J. Granwehr and W. Köckenberger, Appl. Magn. Reson. **34**, 355 (2008).
[14] Y. Hovav, I. Kaminker, D. Shimon, A. Feintuch, D. Goldfarb, and S. Vega, Phys. Chem. Chem. Phys. **17**, 226 (2015).
[15] B. L. Altshuler, Y. Gefen, A. Kamenev, and L. S. Levitov, Phys. Rev. Lett. **78**, 2803 (1997).
[16] D. M. Basko, I. L. Aleiner, and B. L. Altshuler, Ann. Phys. (Amsterdam) **321**, 1126 (2006).
[17] R. Nandkishore and D. A. Huse, Annu. Rev. Condens. Matter Phys. **6**, 15 (2015).
[18] F. Alet and N. Laflorencie, C. R. Phys. **19**, 498 (2018).
[19] D. A. Abanin, E. Altman, I. Bloch, and M. Serbyn, Rev. Mod. Phys. **91**, 021001 (2019).
[20] A. Beskow and J. Nilsson, Arkiv. Fys. **34**, 561 (1967).
[21] L. Khalfin, Zh. Eksp. Teor. Fiz. Pis'ma Red. **8**, 106 (1968) [JETP Lett. **8**, 65 (1968)].
[22] B. Misra and E. C. G. Sudarshan, J. Math. Phys. (N.Y.) **18**, 756 (1977).
[23] W. M. Itano, D. J. Heinzen, J. J. Bollinger, and D. J. Wineland, Phys. Rev. A **41**, 2295 (1990).
[24] P. Facchi and S. Pascazio, in *Progress in Optics* (Elsevier, New York, 2001), pp. 147–217.
[25] H.-P. Breuer and F. Petruccione, *The Theory of Open Quantum Systems* (Oxford University Press, New York, 2002).
[26] D. A. Huse, R. Nandkishore, F. Pietracaprina, V. Ros, and A. Scardicchio, Phys. Rev. B **92**, 014203 (2015).
[27] I. Rodríguez-Arias, M. Müller, A. Rosso, and A. De Luca, Phys. Rev. B **98**, 224202 (2018).
[28] F. Nathan and M. S. Rudner, Phys. Rev. B **102**, 115109 (2020).
[29] G. Kiršanskas, M. Franckié, and A. Wacker, Phys. Rev. B **97**, 035432 (2018).
[30] E. Kleinherbers, N. Szpak, J. König, and R. Schützhold, Phys. Rev. B **101**, 125131 (2020).
[31] A. Abragam and M. Goldman, Rep. Prog. Phys. **41**, 395 (1978).
[32] S. A. Smith, W. E. Palke, and J. T. Gerig, Concepts Magn. Reson. **4**, 107 (1992).
[33] F. Bloch, Phys. Rev. **70**, 460 (1946).
[34] V. Atsarkin, Zh. Eksp. Teor. Fiz. **58**, 1884 (1970) [Sov. Phys. JETP **31**, 1012 (1970)].
[35] See Supplemental Material at http://link.aps.org/supplemental/10.1103/PhysRevLett.126.120603 for technical derivations, complementary numerical results and discussions of the minimal ingredients of the model, which includes Refs. [36–47].
[36] N. Pottier, *Nonequilibrium Statistical Physics: Linear Irreversible Processes* (Oxford University Press, New York, 2010).
[37] I. Rodríguez-Arias, A. Rosso, and A. D. Luca, Magn. Reson. Chem. **56**, 689 (2018).
[38] P. Coleman, *Introduction to Many-Body Physics* (Cambridge University Press, Cambridge, England, 2015).
[39] F. Caracciolo, M. Filibian, P. Carretta, A. Rosso, and A. D. Luca, Phys. Chem. Chem. Phys. **18**, 25655 (2016).
[40] S. C. Serra, M. Filibian, P. Carretta, A. Rosso, and F. Tedoldi, Phys. Chem. Chem. Phys. **16**, 753 (2014).
[41] H. Mizuno, H. Shiba, and A. Ikeda, Proc. Natl. Acad. Sci. U.S.A. **114**, E9767 (2017).
[42] L. Wang, A. Ninarello, P. Guan, L. Berthier, G. Szamel, and E. Flenner, Nat. Commun. **10**, 26 (2019), .
[43] M. Filibian, S. C. Serra, M. Moscardini, A. Rosso, F. Tedoldi, and P. Carretta, Phys. Chem. Chem. Phys. **16**, 27025 (2014).
[44] M. Filibian, E. Elisei, S. C. Serra, A. Rosso, F. Tedoldi, A. Cesàro, and P. Carretta, Phys. Chem. Chem. Phys. **18**, 16912 (2016).
[45] L. F. Chibotaru, A. Ceulemans, and H. Bolvin, Phys. Rev. Lett. **101**, 033003 (2008).
[46] N. W. Ashcroft and N. D. Mermin, *Solid State Physics* (Holt, Rinehart and Winston, 1976).
[47] L. D. Landau and E. M. Lifshitz, *Theory of Elasticity* (Elsevier, New York, 1986).
[48] R. Alicki, Phys. Rev. A **40**, 4077 (1989).
[49] R. Alicki, D. Gelbwaser-Klimovsky, and G. Kurizki, arXiv:1205.4552.
[50] J. S. Lee and J. Yeo, arXiv:2011.00735.
[51] F. Nathan and M. S. Rudner, arXiv:2011.04574.
[52] Y. Hovav, A. Feintuch, and S. Vega, Phys. Chem. Chem. Phys. **15**, 188 (2013).
[53] J. Bezanson, A. Edelman, S. Karpinski, and V. B. Shah, SIAM Rev. **59**, 65 (2017).
[54] Y. Saad, *Iterative Methods for Sparse Linear Systems* (Society for Industrial and Applied Mathematics, University City, PA, 2003).
[55] Y. Li, X. Chen, and M. P. A. Fisher, Phys. Rev. B **98**, 205136 (2018).
[56] A. Chan, R. M. Nandkishore, M. Pretko, and G. Smith, Phys. Rev. B **99**, 224307 (2019).
[57] B. Skinner, J. Ruhman, and A. Nahum, Phys. Rev. X **9**, 031009 (2019).
[58] M. Szyniszewski, A. Romito, and H. Schomerus, Phys. Rev. B **100**, 064204 (2019).
[59] X. Turkeshi, R. Fazio, and M. Dalmonte, Phys. Rev. B **102**, 014315 (2020).
[60] C.-M. Jian, Y.-Z. You, R. Vasseur, and A. W. W. Ludwig, Phys. Rev. B **101**, 104302 (2020).

[61] A. Zabalo, M. J. Gullans, J. H. Wilson, S. Gopalakrishnan, D. A. Huse, and J. H. Pixley, Phys. Rev. B **101**, 060301(R) (2020).
[62] Y. Bao, S. Choi, and E. Altman, Phys. Rev. B **101**, 104301 (2020).
[63] L. Zhang, J. A. Reyes, S. Kourtis, C. Chamon, E. R. Mucciolo, and A. E. Ruckenstein, Phys. Rev. B **101**, 235104 (2020).
[64] X. Cao, A. Tilloy, and A. D. Luca, SciPost Phys. **7**, 24 (2019).
[65] Q. Tang and W. Zhu, Phys. Rev. Research **2**, 013022 (2020).
[66] S. Goto and I. Danshita, Phys. Rev. A **102**, 033316 (2020).
[67] Y. Fuji and Y. Ashida, Phys. Rev. B **102**, 054302 (2020).
[68] *Hopping Transport in Solids*, edited by M. Pollak and B. Shklovskii, Modern Problems in Condensed Matter Sciences, Vol. 28 (Elsevier, New York, 1991).
[69] V. S. Shchesnovich and V. V. Konotop, Phys. Rev. A **81**, 053611 (2010).
[70] P. Barmettler and C. Kollath, Phys. Rev. A **84**, 041606(R) (2011).
[71] D. A. Zezyulin, V. V. Konotop, G. Barontini, and H. Ott, Phys. Rev. Lett. **109**, 020405 (2012).
[72] H. Fröml, A. Chiocchetta, C. Kollath, and S. Diehl, Phys. Rev. Lett. **122**, 040402 (2019).
[73] P. E. Dolgirev, J. Marino, D. Sels, and E. Demler, Phys. Rev. B **102**, 100301(R) (2020).
[74] A. J. Bray and M. A. Moore, Phys. Rev. Lett. **49**, 1545 (1982).
[75] S. Chakravarty, Phys. Rev. Lett. **49**, 681 (1982).
[76] A. Schmid, Phys. Rev. Lett. **51**, 1506 (1983).
[77] A. J. Leggett, S. Chakravarty, A. T. Dorsey, M. P. A. Fisher, A. Garg, and W. Zwerger, Rev. Mod. Phys. **59**, 1 (1987).
[78] L. F. Cugliandolo, D. R. Grempel, G. Lozano, H. Lozza, and C. A. da Silva Santos, Phys. Rev. B **66**, 014444 (2002).